Published in final edited form as:
Neurosurgery. 2010 April ; 66(4): 751–757. doi:10.1227/01.NEU.0000367452.37534.B1.

Firefly Luciferase–Based Dynamic Bioluminescence Imaging: A Noninvasive Technique to Assess Tumor Angiogenesis

Amy Sun, BS[*],
Department of Biological Sciences, Stanford University School of Medicine, Stanford, California

Lewis Hou, MD[*],
Department of Neurosurgery, Stanford University School of Medicine, Stanford, California

Tiffany Prugpichailers, BS,
Department of Biological Sciences, Stanford University School of Medicine, Stanford, California

Jason Dunkel, BS,
Department of Biological Sciences, Stanford University School of Medicine, Stanford, California

Maziyar A. Kalani, BS,
Department of Neurosurgery, Stanford University School of Medicine, Stanford, California

Xiaoyuan Chen, PhD,
Department of Radiology, Stanford University School of Medicine, Stanford, California

M. Yashar S. Kalani, MD, PhD, and
Department of Neurosurgery; Institute for Stem Cell Biology and Regenerative Medicine; and Institute for Neuro-Innovation and Translational Neurosciences, Stanford University School of Medicine, Stanford, California, Current Address: Department of Neurosurgery, Barrow Neurological Institute, Phoenix, Arizona

Victor Tse, MD, PhD
Department of Neurosurgery, Stanford University School of Medicine, Stanford, California, Current Address: Division of Neurosurgery, The Kaiser Permanente Medical Group, Redwood City, California

Abstract

OBJECTIVE—Bioluminescence imaging (BLI) is emerging as a cost-effective, high-throughput, noninvasive, and sensitive imaging modality to monitor cell growth and trafficking. We describe the use of dynamic BLI as a noninvasive method of assessing vessel permeability during brain tumor growth.

METHODS—With the use of stereotactic technique, 10^5 firefly luciferase–transfected GL26 mouse glioblastoma multiforme cells were injected into the brains of C57BL/6 mice (n = 80). After intraperitoneal injection of D-luciferin (150 mg/kg), serial dynamic BLI was performed at 1-minute intervals (30 seconds exposure) every 2 to 3 days until death of the animals. The maximum

Reprint requests: Victor Tse, MD, PhD, Division of Neurosurgery, The Kaiser Permanente Medical Group, Redwood City, CA 94063. tsevictor@gmail.com.
[*]These authors contributed to this work equally.

Disclosures
This project was partially funded by the VPUE Faculty Grant and quarterly grants from Stanford University Undergraduate Research Programs. The authors have no personal financial or institutional interest in any of the drugs, materials, or devices described in this article.

intensity was used as an indirect measurement of tumor growth. The adjusted slope of initial intensity (I_{90}/I_m) was used as a proxy to monitor the flow rate of blood into the vascular tree. Using a modified Evans blue perfusion protocol, we calculated the relative permeability of the vascular tree at various time points.

RESULTS—Daily maximum intensity correlated strongly with tumor volume. At postinjection day 23, histology and BLI demonstrated an exponential growth of the tumor mass. Slopes were calculated to reflect the flow in the vessels feeding the tumor (adjusted slope = I_{90}/I_m). The increase in BLI intensity was correlated with a decrease in adjusted slope, reflecting a decrease in the rate of blood flow as tumor volume increased ($y = 93.8e^{-0.49}$, $R^2 = 0.63$). Examination of calculated slopes revealed a peak in permeability around postinjection day 20 (n = 42, $P < .02$ by 1-way analysis of variance) and showed a downward trend in relation to both postinjection day and maximum intensity observed; as angiogenesis progressed, tumor vessel caliber increased dramatically, resulting in sluggish but increased flow. This trend was correlated with Evans blue histology, revealing an increase in Evans blue dye uptake into the tumor, as slope calculated by BLI increases.

CONCLUSION—Dynamic BLI is a practical, noninvasive technique that can semiquantitatively monitor changes in vascular permeability and therefore facilitate the study of tumor angiogenesis in animal models of disease.

Keywords

Angiogenesis; Dynamic bioluminescence imaging; Luciferase; Tumor

Angiogenesis, the growth of new blood vessels from preexisting vasculature, is important for solid tumor growth to allow the transfer of oxygen, nutrients, and waste.[1,2] Excessive tumor cell proliferation, characteristic of most cancerous growths, is insufficient for a tumor to have physiologic detriment.[1,3] Early studies showed that tumors implanted into a site of little blood circulation, such as the anterior chamber of the eye, fail to grow larger than 1 mm in diameter. However, if the tumor is implanted near the iris, where there is ample blood flow, the tumor grows 16 000 times in size within 2 weeks.[4] Angiogenesis is also positively correlated with metastasis, and metastasis is rare in the absence of new vasculature.[5–7]

Despite the importance of angiogenesis to neoplastic growth and metastasis, there are few noninvasive, in vivo methodologies to monitor angiogenic progression. One such method for calculating blood volume, perfusion, and vascular permeability uses dynamic contrast-enhancing magnetic resonance imaging (MRI).[8] Using dynamic contrast-enhancing MRI, Lüdemann et al[8] could distinguish between glioma grades and types of brain tumors. Other studies suggest that neovascularization during angiogenesis includes an increase in the permeability of the blood-brain barrier, resulting in an increase in intensity during contrast MRI, and is correlated to exponential tumor growth, increased expression of angiogenic factors such as vascular endothelial growth factor and angiopoietin-1 and -2, as well as an increase in vessel caliber and density.[9]

Another available noninvasive in vivo imaging technique takes advantage of the firefly luciferase–transfected brain tumor cell lines. In vivo bioluminescence imaging (BLI), while not practical in patients, is a high-throughput and sensitive imaging modality, making it an excellent tool for monitoring tumor growth and the progress of antitumor therapies in animal models. The substrate, D-luciferin, is known to cross cell membranes and penetrate the blood-brain barrier after intraperitoneal injection into mice, and the excitation photons emitted are detectable through bone, allowing for BLI of any organ, including the brain. Burgos et al[10] used BLI to compare growth curves of brain tumors in orthotopic and heterotopic mice.

In this study, we combine dynamic BLI (DBLI) with histology and illustrate that this noninvasive in vivo technique can be used to monitor tumor growth and permeability of the blood-brain barrier in an experimental model of glioma in mice. Although this imaging modality is currently impractical to use in patients, the technique can be used to study the effects of antiangiogenic therapeutics in animal models.

MATERIALS AND METHODS

Glioblastoma Multiforme Tumor Line

A murine-derived GL26 glioblastoma cell line was used in this study. This cell line originates from a primary mouse brain tumor that was induced in the brains of C57BL/6 mice after intracerebral implantation of methylcholanthrene pellets.[9] The cells were maintained in standard culture conditions using Dulbecco's modified Eagle's medium (high glucose) with 10% fetal calf serum (Invitrogen Corp, Carlsbad, CA) and 1% penicillin-streptomycin antibiotic (Invitrogen Corp) in 5% CO_2 at 37°C. After transfection and selection, 100μg/mL of geneticin (G418) antibiotic (Invitrogen Corp) was added to maintain selection for the expression of the luciferase gene.

Transfection Protocol

Transfection of GL26 with pcDNA3.1-Fluc, in which firefly luciferase expression is driven by a cytomegalovirus promoter, was performed using Lipofectamine 2000 (Invitrogen Corp) according to the manufacturer's protocol. Transfected cells were cultured in the Dulbecco's modified Eagle's medium cocktail, as described above, containing 800 μg/mL of G418 at a concentration for luciferase gene expression selection. Three weeks afterward, light emission of drug-resistant clones was determined by charge-coupled device camera (Xenogen IVIS; Caliper Life Sciences, Hopkinton, MA) to screen for the reporter gene expression. Positive clones were selected and further amplified. The stable cell line is referred to as GL26-(f)luc.

Orthotopic Brain Tumor Model

All animal experiments were conducted according to the surgical protocol approved by the Administrative Panel on Laboratory Animal Care at Stanford University. Six-week old C57BL/6-NBL6 mice (20–25 g) were anesthetized with intraperitoneal injections of avertin solution, composed of 1.2% 2,2,2-tribromoethanol (Sigma-Aldrich, St Louis, MO) in 1.2% tertamyl alcohol (Fisher Scientific, Pittsburgh, PA) and 0.9% NaCl, using standard protocol. Animals were continuously monitored through neurologic stimulation of hind paws and respiration rate. A warming blanket maintained the body temperature of the mice during anesthetization. Mice were placed onto a stereotactic frame (Kopf Instruments, Tujunga, CA) and secured by ear-bars. Under a dissection microscope, a 1-cm parasagittal incision was made to expose the coronal and superior sagittal sinus. An electric dental drill was used to create a 1-mm-diameter burr hole 2 mm lateral and 1 mm posterior to the anatomic bregma over the right hemisphere. A 2-μL suspension containing low-passage (<17 passages) 10^5 GL26-luc cells was prepared in serum-free Dulbecco's modified Eagle's medium (low glucose). After dural penetration, cells were injected 2.5 mm into the parenchyma using a 10-μL microinjector syringe (Hamilton Co, Reno, NV) at a rate of 1μL/min. The needle was then retracted 1 mm/min, and the scalp was closed using 5-0 Vicryl sutures (Ethicon, Inc, Somerville, NJ). This model was previously described in the literature and has been shown to result in up to 90% engraftment with consistent tumor size and growth.[9,11,12] Tumor volume was estimated by (length squared × width)/2, where length was the longer measurement. Weight was measured by AG204 DeltaRange balance (Mettler-Toledo, Columbus, OH).

Bioluminescence Imaging

Intracranial tumor growth was monitored using DBLI using the Xenogen IVIS 200 imaging system (Caliper Life Sciences). Mice were anesthetized by inhalation of 1% to 2% isofluorane (Aerrane; Baxter Healthcare Corp, Deerfield, IL) and given intraperitoneal injections of 200 μL D-luciferin (150 mg/kg; catalog no. L8220; Biosynth AG, Staad, Switzerland). Each set of mice received injections within 45 seconds and in the same order. Serial images were taken using Living Image software (Caliper Life Sciences) every 2 or 3 days once the presence of tumor was confirmed. Sequential images measuring the bioluminescent activity of the luciferase enzyme were acquired at 1-minute intervals (30 seconds exposure, no time delay) for at least 20 minutes. The luminescent camera was set to 30 seconds exposure, medium binning, 1 f/stop, blocked excitation filter, and open emission filter. The photographic camera was set to 2 seconds exposure, medium binning, and 8 f/stop. Field of view was set to 22 cm to image 5 mice at once. Identical settings were used to acquire each image and region of interest.

Permeability Calculation

Data on regions of interest were obtained from the Living Image software and imported into Microsoft Office Excel (Microsoft Corp, Redmond, WA). Calculations were made to determine the rate of luminescence, which is directly correlated to luciferase enzyme function and limited by rate of D-luciferin uptake from the blood supply. Intensity of light emission at the first time interval (I_{90}) (approximately 90 seconds after injection of D-luciferin) was identified. Similarly, magnitude and timing of maximal intensity (I_m) was also noted. Calculated or adjusted slope was defined as the ratio of I_{90} to I_m (I_{90}/I_m), allowing for compensation of changes in tumor size. One-way analysis of variance examined the statistical significance of the peak permeability trend observed. Graphs in Excel and MatLab (The MathWorks, Inc, Natick, MA) were constructed to follow the permeability profile of mice.

Evans Blue Permeability Analysis

Mice were imaged according to the methodology described above and killed on the basis of the permeability profile. A modified Evans blue dye protocol was used to assess the vessel permeability.[13] Evans blue dye ($C_{34}H_{24}N_6O_{14}S_4Na_4$), 2% wt/vol in phosphate-buffered saline (Invitrogen Corp), was injected into the external jugular vein. Within 1 minute, mice were subsequently perfused with phosphate-buffered saline and 4% paraformaldehyde. Brains were harvested, and tumors were dissected out. Normal brain parenchyma from the contralateral lobe of the tumor was used as control. Concentration of Evans blue dye was measured in brain tumor extracts using spectrophotometry (620/635 nm). Tumor tissue dye concentration (μg of dye per g of tissue) was normalized by weight and dye concentration on the contralateral side of the brain. Linear correlation was established between Evans blue analysis and DBLI permeability analysis.

Histology

Mice were perfused with phosphate-buffered saline and 4% paraformaldehyde at prepeak, peak, and postpeak permeability. Harvested brains were placed in 30% sucrose solution for 3 days. Brains were frozen and cut into 30-μm serial sections using a cryostat microtome (Microm HM450; Thermo Fisher Scientific, Waltham, MA). Sections were mounted on slides and counterstained with Vectashield mounting medium (Vector Laboratories, Burlingame, CA) containing 4′,6-diamidino-2-phenylindole (Vector H-1500) for nuclear detection. Tumor vessels were visualized with CD31 antibody (dilution 1:100). Slides were viewed with an Axioplan2 Zeiss fluorescence microscope, Axioskop (with preset 4′,6-diamidino-2-phenylindole and CY3 filters), and a Zeiss LSM510 confocal microscope (Carl

Zeiss, Inc, Thornwood, NY). Regions of tumor growth were identified by a dense 4′,6-diamidino-2-phenylindole nuclear staining pattern. Specimens were examined under low- (×200) and high-power fields (×400). At least 6 random fields (150 × 150 mm^2) were examined per slide. Each field was divided into 4 quadrants. Two replicate slides per animal were examined for each staining combination. Areas defined for analyses were predetermined empirically from previous studies to optimize the best representation of blood vessel distribution within tumor sections.[14] Figure images were digitally assembled with Adobe Photoshop (Adobe Systems, Inc, San Jose, CA).

RESULTS

DBLI Intensities and Vascular Densities Increase Over the Time Course of the Experiment

Tumor-implanted animals were sequentially imaged using DBLI on alternative days as described under Materials and Methods. Starting on day 15, DBLI consistently exhibited increased signal intensities. The signal intensity continued to increase during the course of the experiment until the demise of the animals (Fig. 1A). As scanning time was increased from 2 to 20 minutes, nearly all time points exhibited an overall increase in the observed signal intensities. Overlaid time-course intensity curves spanning multiple imaging days suggest that as postinjection day increased, the time to reach maximum intensity decreased (Fig. 1B). The day 23 time point reached an asymptotic peak at 12 minutes, after which signal intensities began to diminish (Fig. 1B). To show that maximum intensity is directly correlated with tumor size, mice were killed on the day of imaging, and their estimated tumor volume (length squared × width)/2, where length was the longer measurement) was compared with the maximum intensity observed that day. We were able to show a strong linear correlation between tumor growth and maximum intensity ($R^2 = 0.93$) (Fig. 1C). Mice injected with nontransfected cells or with no cells resulted in no signal in comparison to background (data not shown). The vascular density similarly increased with time and reached an asymptotic peak at postinjection days 23 to 26 (Fig. 1D), corresponding to the period of the exponential growth of the tumor (Fig. 1E). We further studied this increase in vascular density by evaluating the caliber of the vessels generated over the time course of the experiment and observed an increase in the vascular caliber (day 15, 11.9 ± 1.8 μm; day 20, 19.3 ± 1.5 μm; day 25, 18.8 ± 2.5 μm; day 30, 19.6 ± 1.6 μm; $P < .04$) (Fig. 1F). After day 28, there was a resegregation of the average vessel caliber into small and larger vessels (Fig. 1, G–L).

Tumor Signal Intensity Is Inversely Related to the Adjusted Intensity

To assess vascular flow, we measured the magnitude and timing of maximal intensity and correlated this to the adjusted intensity, which was measured as the ratio of the flow in the initial 90 seconds relative to the maximal intensity. This adjusted intensity allowed for compensation for changes in tumor size over the course of the experiment. The ratio of I_m to I_{90}/I_m decreased over the time course of the experiment ($y = 93.8e^{-0.49}$, $R^2 = 0.63$) (Fig. 2).

The Concentration of Evans Blue Correlates Positively With the Tumor Signal Intensity

To further assess the integrity of DBLI intensities as a measure of permeability, we correlated the rate of Evans blue uptake to the adjusted signal intensity. Over the studied time points, an increase in the Evans blue concentration in the tissue correlated with an increased tumor intensity ($y = 181.32x + 6.57$; $R^2 = 0.58$) (Fig. 3).

DISCUSSION

As solid tumors grow, they depend on the formation of new blood vessels to meet the increased metabolic demands of uncontrolled proliferation. It is now well known that

important signaling molecules control this intricate process, which results in increased delivery of blood and nutrients and removal of wastes from the tumor mass. Angiogenesis in the brain is particularly intricate, since new vessel formation frequently results in increased permeability and disruption of the blood-brain barrier. The disruption of the blood-brain barrier allows for the enhanced delivery of drugs that usually would have little permeability to the brain as well as allowing for the identification of the tumor mass using contrast agents.

In this study, we used DBLI with D-luciferin to monitor tumor growth in an animal model of glioma. It is important to note there are other invasive and noninvasive methods to assess vascular permeability and arrive at some of the conclusions in this article. Several groups have used various MRI modalities, including quantitative measurement with double-echo dynamic MRI,[15,16] perfusion computed tomography,[17] positron emission tomography, and thermodilution methods[18] in various clinical settings to assess vascular architecture and vascular permeability. Each method has advantages and disadvantages (Table 1), but, fundamentally, all of these methods look at diffusion and change in position of tracers to arrive at parameters for permeability, stasis, and flow. Using the current method, we observed an increase in the DBLI intensities over the course of the experiment (Fig. 1, A and B). The increased intensities correlate with increased tumor mass (Fig. 1C) and reflect the dynamic of vascular changes associated with tumor angiogenesis (Fig. 3). The DBLI intensities continued to increase for all time points until days 23 to 25. Between days 23 and 25, one reaches an asymptote of intensities at $T = 12$ minutes. This may be explained by increased clearance of the D-luciferin from the tumor mass, most likely owing to increased flow and relatively intact permeability of the tumor vessels. As the tumor continued to grow over the course of the experiment (Fig. 1E), we observed a concomitant increase in vascular density (Fig. 1D, vascular caliber (Fig. 1F), and permeability. In the later phase of tumor growth, the vessels became more leaky and took on a sinusoidal appearance resulting, in stagnancy of flow (Fig. 2). After day 28, there was a general redistribution of vascular caliber (Fig. 1F). This is attributable to involution of the vessels within the tumor mass and the proliferation of smaller-caliber vessels at the advancing edge of the tumor.

To assess the flow in the tumor vessels, we plotted the maximal intensity of DBLI signals relative to the adjusted intensities and noted that, as I_m increased, the ratio of I_{90}/I_m decreased. This suggests that within the initial 90 seconds, the flow is sluggish, as depicted by the diminished I_{90}/I_m ratio. Gradually, the flow increases, most likely owing to increased number and caliber of blood vessels, and this results in an increased I_m. The decrease in the adjusted intensities and subsequent increase in the ratio of I_m to (I_m/I_{90}) is consistent with sluggish flow and leakiness of the tumor over the time course of the experiment (Fig. 2).

To provide a well-established control and to assess the integrity of the DBLI intensities as readout for tumor vessel permeability, we carried out Evans blue staining of the tumor vessels over the same time points as in our experiments. We noted a negative correlation between the concentration of Evans blue reagent in the tumor mass and the adjusted intensities, consistent with sluggish flow in the tumor vessels over the time points of the experiment (Fig. 3).

CONCLUSIONS

In vivo assessment of tumor angiogenesis is crucial for studying tumor progression and the administration of antiangiogenesis-based therapy. The onset of angiogenesis is characterized by an increase in vessel permeability, which is thought to be necessary for the recruitment of endothelial progenitor cells and the establishment of extravascular scaffold. DBLI is a practical, noninvasive technique to monitor the blood flow through the vascular tree and into

the tumor tissue. Although currently impractical for use in patients, this study and others like it suggest that DBLI has great utility for monitoring tumorigenesis in animal models of disease. Our study shows that DBLI intensities correlate well with tumor growth. Tumor growth is positively correlated with increased adjusted intensities and the ratio of maximal intensity to the adjusted intensities is diminished, suggesting increased, albeit sluggish, blood flow into the tumor mass as the tumor grows. A comparison of the Evans blue method to the DBLI negatively correlates Evans blue concentration in tumor tissue to the adjusted intensities, suggesting that DBLI can be used as a reliable noninvasive in vivo method to study and assess tumor growth.

Acknowledgments

M. Yashar S. Kalani, MD, PhD, is a fellow of the Hanbery Neurosurgical Society. Vincent Mei and Yao Yu generated the slope and maximum intensity curves using MatLab software. Lewis Hou, MD, is a Neurosurgical Research Foundation Resident Fellow 2006-2008.

ABBREVIATIONS

BLI	bioluminescence imaging
DBLI	dynamic bioluminescence imaging
I_m	maximal intensity
I_{90}	intensity at 90-second time interval
MRI	magnetic resonance imaging

COMMENT

In this report, the authors extend and expand on previously published work that has used bioluminescent imaging (BLI) as a measure of tumor growth. They are able to show that dynamic BLI (ie, imaging over a period of time) reflects tumor growth, but, most interestingly, they suggest that it also correlates with blood vessel density and diameter. This shows that the technique may be useful for the study of neoangiogenesis, although it still needs refinement. The major issues are: (1) the increase in vessel density is not linear (see Fig. 1D in the article), and, thus, the interpretation of changes in BLI may require additional time points and animals to provide such a correlation; (2) BLI is not a direct measure of vascularity, but, rather, of viable tumor cells; and (3) only 1 cell line was studied, and whether these findings can be generalized to others will require more work. Ultimately, though, the application of imaging modalities such as dynamic BLI can only be of help in preclinical translational therapies, and the authors should be encouraged to continue pushing this line of research.

E. Antonio Chiocca

Columbus, Ohio

REFERENCES

1. Kerbel RS. Tumor angiogenesis. N Engl J Med. 2008; 358(19):2039–2049. [PubMed: 18463380]
2. Folkman J. Tumor angiogenesis: therapeutic implications. N Engl J Med. 1971; 285(21):1182–1186. [PubMed: 4938153]
3. Folkman J. Angiogenesis. Annu Rev Med. 2006; 57:1–18. [PubMed: 16409133]
4. Holleb AI, Folkman J. Tumor angiogenesis. CA Cancer J Clin. 1972; 22(4):226–229. [PubMed: 4625047]

5. Gimbrone MA Jr, Cotran RS, Leapman SB, Folkman J. Tumor growth and neovascularization: an experimental model using the rabbit cornea. J Natl Cancer Inst. 1974; 52(2):413–427. [PubMed: 4816003]
6. Gimbrone MA Jr, Leapman SB, Cotran RS, Folkman J. Tumor dormancy in vivo by prevention of neovascularization. J Exp Med. 1972; 136(2):261–276. [PubMed: 5043412]
7. Gimbrone MA Jr, Leapman SB, Cotran RS, Folkman J. Tumor angiogenesis: iris neovascularization at a distance from experimental intraocular tumors. J Natl Cancer Inst. 1973; 50(1):219–228. [PubMed: 4692862]
8. Lüdemann L, Grieger W, Wurm R, Wust P, Zimmer C. Quantitative measurement of leakage volume and permeability in gliomas, meningiomas and brain metastases with dynamic contrast-enhanced MRI. Magn Reson Imaging. 2005; 23(8):833–841. [PubMed: 16275421]
9. Veeravagu A, Hou LC, Hsu AR, et al. The temporal correlation of dynamic contrast- enhanced magnetic resonance imaging with tumor angiogenesis in a murine glioblastoma model. Neurol Res. 2008; 30(9):952–959. [PubMed: 18662497]
10. Burgos JS, Rosol M, Moats RA, et al. Time course of bioluminescent signal in ortho topic and heterotopic brain tumors in nude mice. Biotechniques. 2003; 34(6):1184–1188. [PubMed: 12813886]
11. Bababeygy SR, Cheshier SH, Hou LC, Higgins DM, Weissman IL, Tse VC. Hematopoietic stem cell-derived pericytic cells in brain tumor angio-architecture. Stem Cells Dev. 2008; 17(1):11–18. [PubMed: 18240955]
12. Hsu AR, Hou LC, Veeravagu A, et al. In vivo near-infrared fluorescence imaging of integrin αvβ3 in an orthotopic glioblastoma model. Mol Imaging Biol. 2006; 8(6):315–323. [PubMed: 17053862]
13. Prabhu SS, Broaddus WC, Oveissi C, Berr SS, Gillies GT. Determination of intracranial tumor volumes in a rodent brain using magnetic resonance imaging, Evans blue, and histology: a comparative study. IEEE Trans Biomed Eng. 2000; 47(2):259–265. [PubMed: 10721633]
14. Tse V, Yung Y, Santarelli JG, et al. Effects of tumor suppressor gene (p53) on brain tumor angiogenesis and expression of angiogenic modulators. Anticancer Res. 2004; 24(1):1–10. [PubMed: 15015569]
15. Gambarota G, Leenders W, Maass C, et al. Characterisation of tumour vasculature in mouse brain by USPIO contrast-enhanced MRI. Br J Cancer. 2008; 98(11):1784–1789. [PubMed: 18506183]
16. Zaharchuk G. Theoretical basis of hemodynamic MR imaging techniques to measure cerebral blood volume, cerebral blood flow, and permeability. AJNR Am J Neuroradiol. 2007; 28(10): 1850–1858. [PubMed: 17998415]
17. Petralia G, Preda L, Giugliano G, et al. Perfusion computed tomography for monitoring induction chemotherapy in patients with squamous cell carcinoma of the upper aerodigestive tract: correlation between changes in tumor perfusion and tumor volume. J Comput Assist Tomogr. 2009; 33(4):552–559. [PubMed: 19638848]
18. Kenner T, Moser M, Hinghofer-Szalkay H. Determination of cardiac output and of transcapillary fluid exchange by continuous recording of blood density. Basic Res Cardiol. 1980; 75(4):501–509. [PubMed: 7436993]

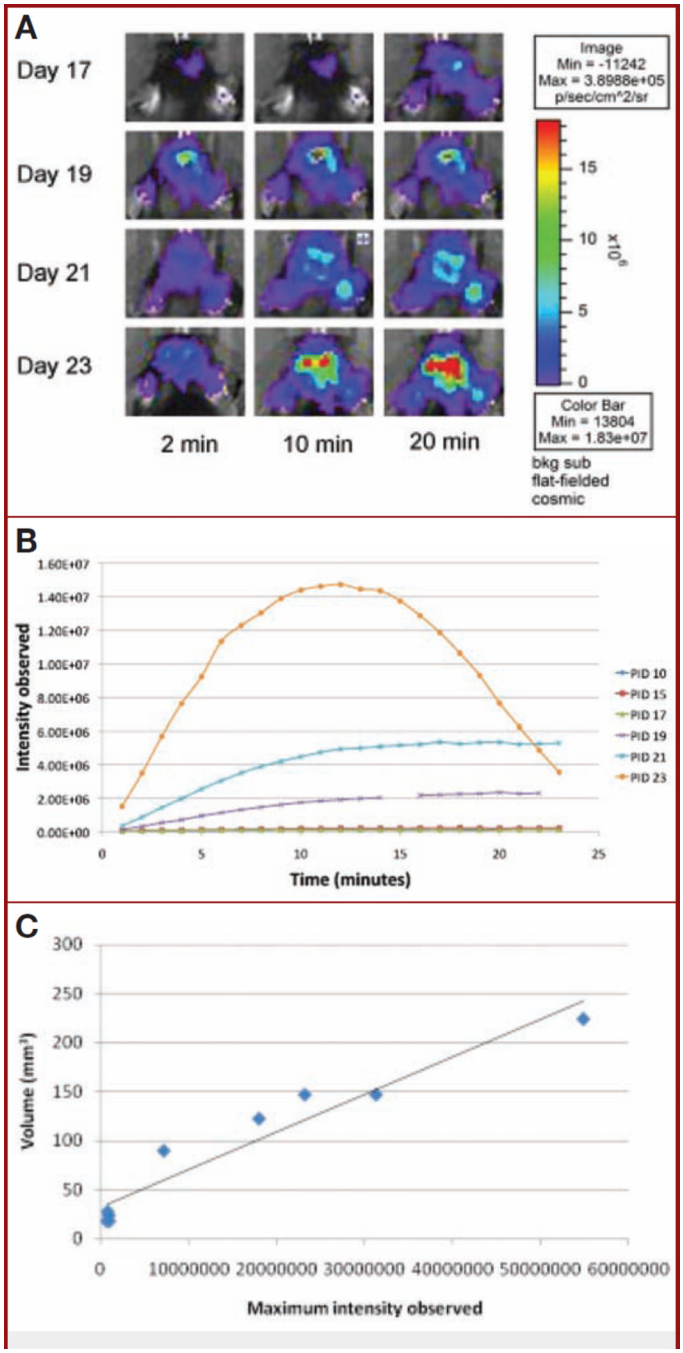

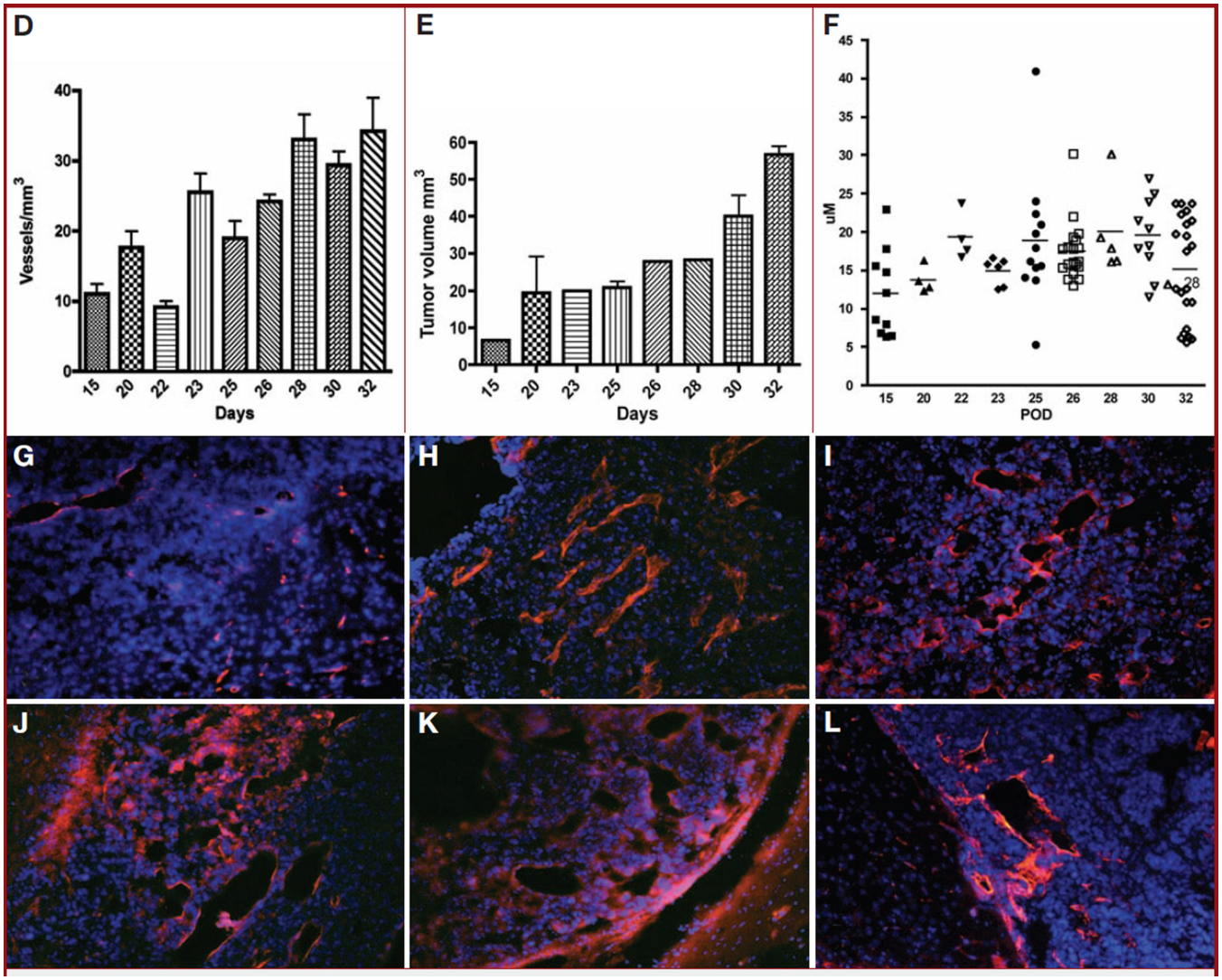

Figure 1.

A, dynamic bioluminescence imaging (DBLI) of orthotopic GL26-luc tumor intensity. Firefly luciferase–transfected GL26-luc cells were stereotactically implanted in the right frontal lobe and imaged on postinjection days (PIDs) 17, 19, 21, and 23. Total flux recorded by Living Image software; pseudocolor image reflects photon flux and not necessarily the perimeter of the tumor. As time after intraperitoneal injection of luciferin increases, tumor intensity increases, as it reaches its maximum. As PID increases, tumor intensity also increases, reflecting tumor growth. **B**, intensity curves of a tumor over the course of an experiment. DBLI images were taken every other day, and observed bioluminescent intensities within regions of interest encompassing the tumor injection site were plotted for each minute. As the tumor grows over time, maximum intensity increases (I_m) and the time to reach I_m (slope) decreases. Minute 15 of PID 19 was removed, owing to abnormally high background levels of intensity. **C**, graph showing correlation of maximum intensity and tumor volume. Tumor volume (estimated by (length squared × width)/2, where length is the longer measurement) is directly related to maximum intensity observed on the day that the animal is killed ($R^2 = 0.93$, n = 9). This strong correlation suggests that bioluminescence imaging is representative of tumor volume. **D**, graph showing that vascular volume density (mm^3) increases over the time points of the experiment. The results of a representative

experiment are shown. **E**, graph showing that tumor volume (mm^3) increases over the time course of the experiment. The results of a representative experiment are shown. **F**, plot showing that vascular caliber (μm) gradually increases from day 0 to day 28 ($P < .04$). POD, postoperative day. **G–L**, representative histologic sections representing tumor growth at various time points (**G**, day 10; **H**, day 15; **I**, day 17; **J**, day 19; **K**, day 21; **L**, day 23) over the course of the experiment, illustrating the observed increase in vascular caliber (blue, nuclei, 4′,6-diamidino-2-phenylindole; red, vascular endothelium, CD31).

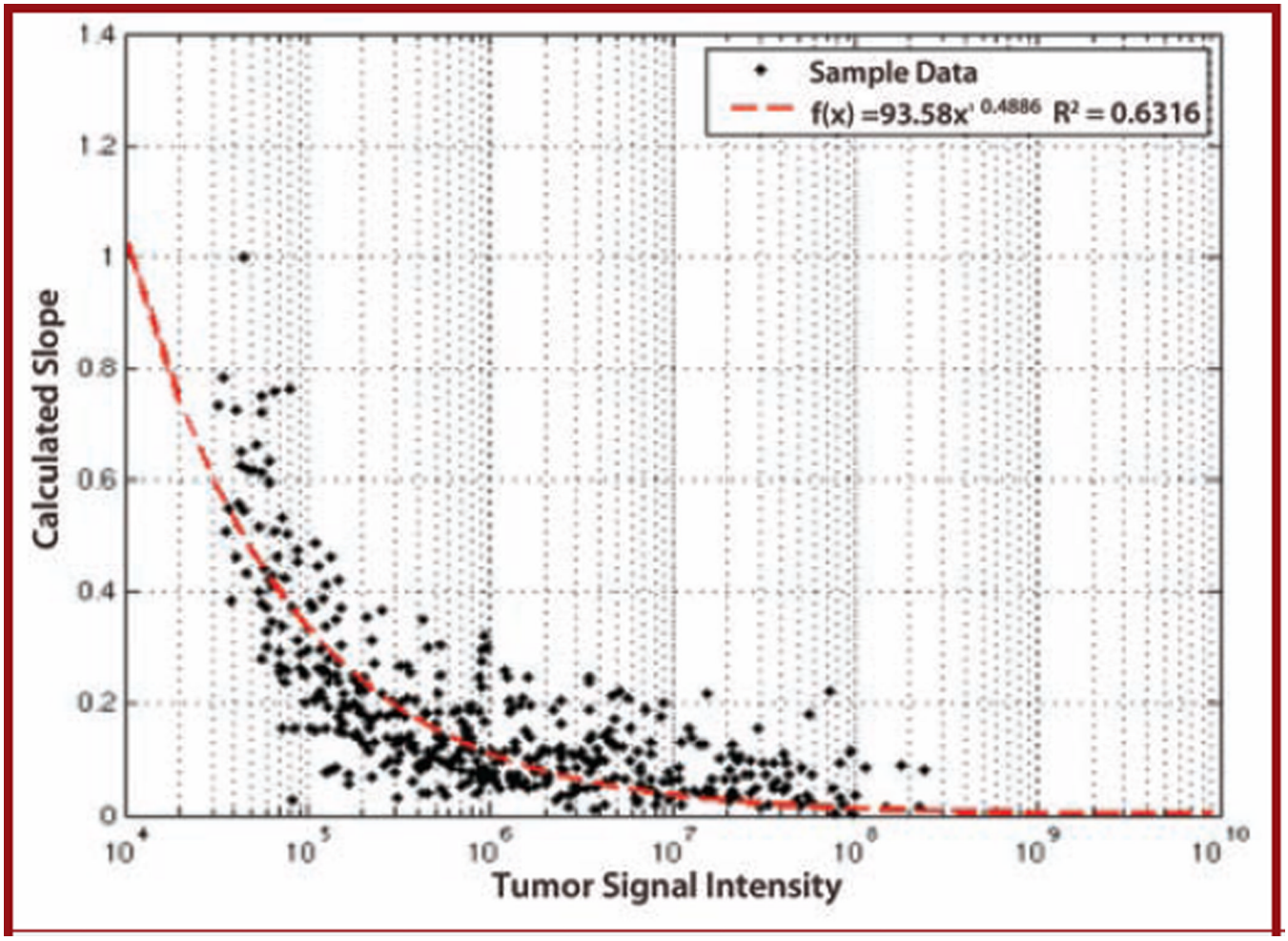

Figure 2.

Graph showing negative correlation between calculated slope and maximum intensity. DBLI slope vs maximum intensity revealed a power function: $y = 93.8x^{-0.49}$, $R^2 = 0.63$. As the tumor increases in size, the calculated slope decreases, revealing an increase in flow into the tumor mass.

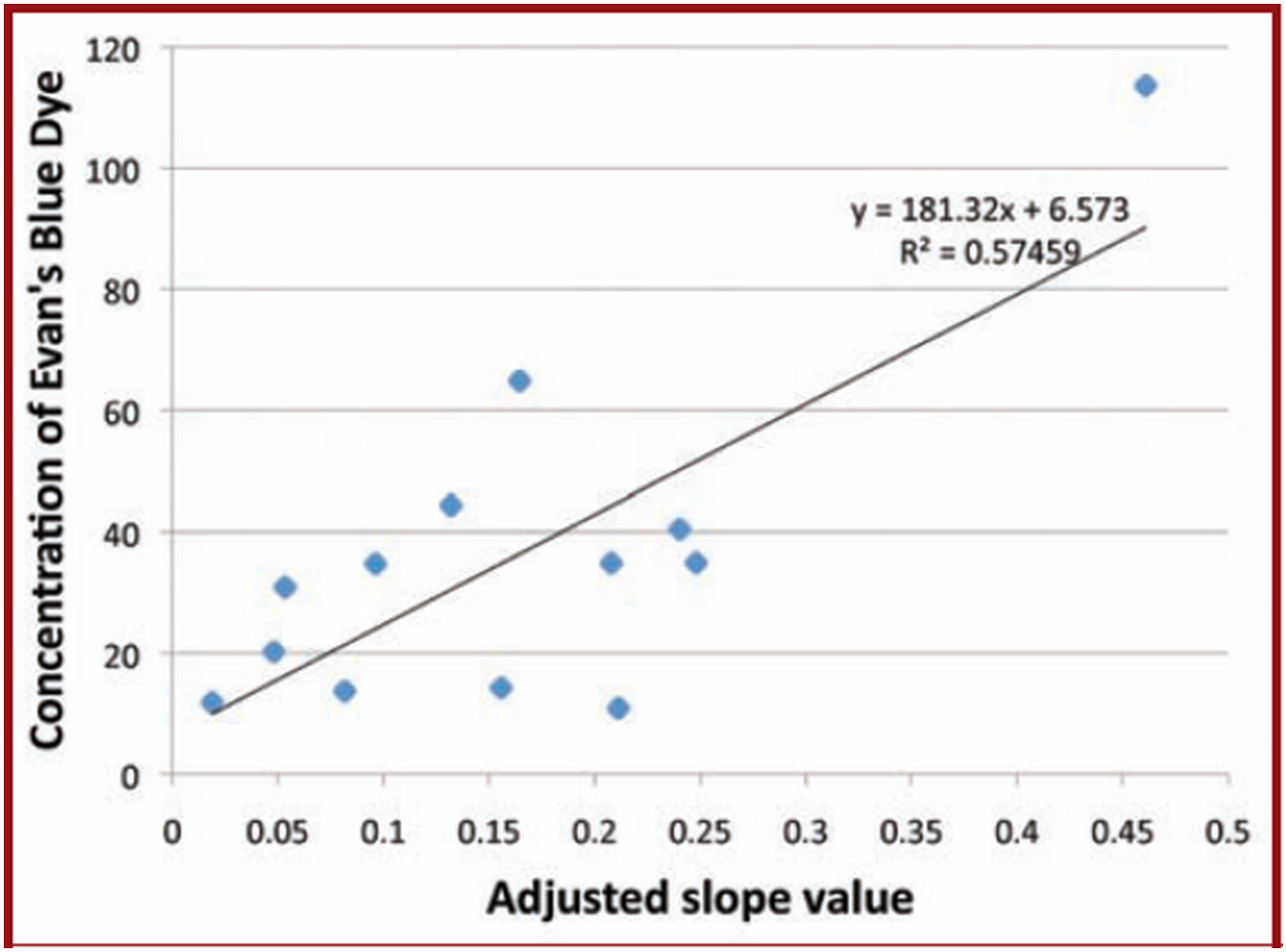

Figure 3.

Graph showing correlation between Evans blue histology and adjusted slope value. The calculated slope correlates linearly with the uptake of Evans blue dye into the tumor tissue. As the slope decreases, the ability of D-luciferin or Evans blue dye to reach the tumor is diminished.

TABLE 1

Advantages and Disadvantages of Various Modalities for Assessing Vascular Permeability.[a]

Method	Advantages	Disadvantages
Echo dynamic MR imaging	Non-invasive; readily available; good visualization of the posterior fossa	High background and low accuracy due to contrast -dosing effects; various methods to process data making cross-institution use difficult; time consuming
Perfusion computed tomography	Non-invasive; rapid; readily available	Poor detail of anatomy of tumor; poor visualization of the posterior fossa; High background and low accuracy due to contrast -dosing effects
Positron emission tomography	Non-invasive; high accuracy (especially when combined with other methods such as MR and CT)	Poor resolution for the brain; expensive; time consuming; few well established protocols for large scale clinical use
Thermodilution		Invasive; expensive; difficult to apply to the brain; inaccurate

[a] CT, computed tomographic; MR, magnetic resonance.